3. A. K. Majumdar, V. S. Pratap, and D. B. Spalding, "Numerical computation of flow in rotating ducts," Trans. ASME, J. Fluids Eng., 99, 148 (1977).
4. R. Simon, R. Schilling, and K. O. Felsch, "Berechnung der ausgebildeten turbulent Strömung in rotierenden Kanälen mit rechteckigem Querschnitt," Stroemungsmech. Stroemungsmasch., No. 28, 33 (1980).
5. J. P. Johnston, "Internal flows," in: Turbulence, P. Bradshaw (ed.), Springer-Verlag, Berlin-New York (1976).
6. J. P. Johnston, R. M. Halleen, and D. K. Lezius, "Effects of spanwise rotation on the structure of two-dimensional fully developed turbulent channel flow," J. Fluid Mech., 56, 533 (1972).
7. B. E. Launder, G. J. Reece, and W. Rodi, "Progress in the development of a Reynolds-stress turbulence closure," J. Fluid Mech., 68, 537 (1975).
8. R. M. C. So, "A turbulence velocity scale for curved shear flows," J. Fluid Mech., 70, 37 (1975).
9. M. M. Gibson, "An algebraic stress and heat-flux model for turbulent shear flow with streamline curvature," Int. J. Heat Mass Transfer, 21, 1609 (1978).
10. V. V. Ris and S. A. Smirnov, "Influence of the entrance conditions on the development of turbulent flow in a rotating channel," in: Structure of Turbulent Flows [in Russian], Minsk (1982).
11. D. K. Lezius and J. P. Johnston, "Roll-cell instabilities in rotating laminar and turbulent channel flows," J. Fluid Mech., 77, 153 (1976).
12. I. A. Hunt and P. N. Joubert, "Effects of small streamline curvature on turbulent duct flow," J. Fluid Mech., 91, 633 (1979).
13. V. K. Shchukin, Heat Exchange and Hydrodynamics of Internal Streams in Mass Force Fields [in Russian], Mashinostroenie, Moscow (1980).
14. E. Döbner, "Über den Strömungswiderstand in einem rotierenden Kanal," Dissertation, Tech. Hochsch. Darmstadt (1959).
15. G. G. Branover and A. B. Tsinober, Magnetohydrodynamics of Incompressible Media [in Russian], Nauka, Moscow (1970).

NUMERICAL STUDY OF LAMINARIZATION EFFECTS IN TURBULENT BOUNDARY LAYERS OF ACCELERATED FLOWS

V. G. Zubkov

UDC 532.514.4

1. Introduction. In a number of experimental data from studies of turbulent flows with acceleration a substantial variation is noted in the characteritics of heat transfer and friction from the corresponding values, obtained from the relations for turbulent flows [1, 2]. The larger the value of the flow acceleration, the more significant the deviation of the integral characteristics of heat transfer and friction, as well as of the profiles of mean velocities and temperature from the universal relations for the turbulent flow regime toward dependences corresponding to the laminar regime. This effect became called laminarization of turbulent flows.

It is possible to estimate the generation condition of laminarization within the first approximation by means of the acceleration parameter $K = (\nu/U_\infty^2)dU_\infty/dx$, characterizing the extent of flow acceleration. It has been established that lowering of the heat transfer parameters starts being noticed in flows with $K > 2 \cdot 10^{-6}$. This parameter, however, does not allow quantitative estimation of effects generated by laminarization.

Account of the variation in the structure of turbulent flows under the action of accelerated flow makes it possible to approach more correctly the projection of various constructions. For example, for an external flow, when the gas flow between turbine blades and in supersonic nozzles an inverse flow transition can cause lowering of heat transfer between the heating gas flow and the construction surface. In heat transfer instruments, when the heat transfer intensity must be largest, a similar effect leads to undesirable results. This gen-

Moscow. Translated from Zhurnal Prikladnoi Mekhaniki i Tekhnicheskoi Fiziki, No. 2, pp. 71-78, March-April, 1985. Original article submitted February 21, 1984.

0021-8944/85/2602-0215$09.50

erates the necessity of creating a calculation result, capable of describing variations in the flow parameters under the action of a negative pressure gradient.

Following Boussinesq, the tangent stress of turbulent friction in planar flow is determined by the relation $-\langle u'v'\rangle = \mu_T \partial U/\partial y$, where μ_T is the coefficient of turbulent momentum exchange. Similarly, one determines the turbulent heat transfer $-C_p\rho\langle v'T'\rangle = \lambda_T \partial T/\partial y$, where λ_T is the coefficient of turbulent heat conductivity, related to μ_T through the turbulent Prandtl number $Pr_T = C_p\mu_T/\lambda_T$. Thus, all difficulties in determining the unknown fluctuating components of the boundary layer equations are shifted to the search of the coefficient μ_T, for whose determination one must employ further hypotheses.

2. Hypothesis of Path Length Mixing. The simplest method of determining μ_T is based on using the hypothesis of path length mixing, suggested by Prandtl

$$\mu_T = \rho l^2 |\partial U/\partial y|. \tag{2.1}$$

In the external boundary layer region the path length mixing l is proportional to the boundary layer thickness $l = \beta\delta$. In the immediate neighborhood of the streamline surface l is assumed proportional to the transverse coordinate, and by means of the correction introduced by Van Driest [3] is determined by the equation

$$l = ky\left[1 - \exp\left(-y_*/A_+^0\right)\right], \tag{2.2}$$

where $A_+^0 = 26$ is the Van Driest constant.

The system of differential equations, closed on the basis of the hypothesis of path length mixing and describing the turbulent boundary layer, was solved in the present study by a finite difference method. The validity of this turbulence model in describing laminarization effects was estimated by comparing the calculations with the experimental data of [1] (Fig. 1, where the points are experiment, and curve 1 corresponds to calculations). It follows from Fig. 1 that in the flow acceleration region the calculated values of the Stanton number significantly exceed the experimental values.

If the parameter A_+ in Eq. (2.2) is interpreted as a dimensionless viscous sublayer thickness, in the region of acceleration action, where, according to experimental data, the relative viscous sublayer thickness increases, the value of the parameter A_+ must also increase. In the present study we analyzed the following dependences of the parameter A_+ on the amount of flow acceleration:

$$A_+ = A_+^0 \sqrt{\tau/\tau_{st}}\left(1 + 11.8P^+\right)^{-1/2} \quad [4]; \tag{2.3}$$

$$A_+ = A_+^0\left(1 + 30.18P^+\right)^{-1} \quad [5]; \tag{2.4}$$

$$A_+ = \begin{cases} A_+^0, & L_* \leqslant 1{,}9\cdot 10^3, \\ 11 + 7.9\cdot 10^3 L_*, & L_* > 1{,}9\cdot 10^3 \end{cases} \quad [6], \tag{2.5}$$

where $P^+ = -K(C_f/2)^{-3/2}$ is the dimensionless pressure gradient, and $L_* = KC_f$ is the laminarization parameter.

At the initial stage of flow acceleration the results of performing calculations by using (2.3)-(2.5), curves 2-4 of Fig. 1, coincide with the experimental data. Below the flows, however, as follows from the curves, the deviation between calculation and experiment in the laminarization region increases. This result can be explained as follows. When the action of flow acceleration is discontinued, according to Eqs. (2.3)-(2.5) the parameter A_+ stops varying, and becomes again constant. At the same time the relative viscous sublayer thickness continues increasing until some distance below the flow [7].

3. The $e - \varepsilon$ Turbulence Model. It is more justified to establish the laws regulating the mechanism of turbulent transfer, which allows the idea of connection between the coefficient of bulk turbulence, the kinetic energy of turbulent motion e, and the turbulence scale L, first predicted by Kolmogorov [8], and independently suggested by Prandtl [9]:

$$\mu_T = \rho C_\mu^0 \sqrt{e}\, L. \tag{3.1}$$

The magnitude of the kinetic energy of turbulent motion is determined as a result of solving the differential equation of turbulent intensity, which for the case of stationary planar flow is written in the form

$$\rho U\frac{\partial e}{\partial x}+\rho V\frac{\partial e}{\partial y}=\frac{\partial}{\partial y}\left(\mu\frac{\partial e}{\partial y}\right)-\frac{\partial}{\partial y}[\langle v'(p'+\rho e)\rangle]\ -\rho\langle u'v'\rangle\frac{\partial U}{\partial y}-\rho\varepsilon. \tag{3.2}$$

New unknowns appear, however, with the introduction of (3.1), (3.2), which must be determined from the experimental data so as to achieve closure of the boundary layer equations.

Based on the Kolmogorov similarity hypothesis [10], a connection can be obtained between the values of dissipation and turbulence intensity for the case of large turbulent Reynolds numbers:

$$\varepsilon=\psi e^{3/2}/L. \tag{3.3}$$

In the case of flow with small Reynolds numbers ($R_T = e^2/\nu\varepsilon < 10^3$) the coefficient ψ in Eq. (3.3) is not a constant quantity, but depends on R_T. A similar connection makes it possible to eliminate from consideration the integral turbulence scale, and to determine the coefficient of turbulent exchange from the equation

$$\mu_T=C_\mu\,\mu R_T. \tag{3.4}$$

An additional equation, describing the variation of the magnitude of kinetic energy dissipation of fluctuating motion, is obtained for the case of locally isotropic turbulence by a derivation from the Navier-Stokes equation [11]. The unknown terms of this equation, containing velocity correlation components of second and higher order, are determined by dimensionality considerations and on the basis of experimental data in terms of the mean flow parameters, the turbulence intensity, dissipation, and the closure parameters. For the case of planar stationary flow of a compressible fluid the dissipation equation is written in the form [12]

$$\rho U\frac{\partial\varepsilon}{\partial x}+\rho V\frac{\partial\varepsilon}{\partial y}=\frac{\partial}{\partial y}\left[\left(\mu+\frac{\mu_T}{\sigma_\varepsilon}\right)\frac{\partial\varepsilon}{\partial y}\right]+C_1\mu_T\frac{\varepsilon}{e}\left(\frac{\partial U}{\partial y}\right)^2-C_2\frac{\rho\varepsilon^2}{e}. \tag{3.5}$$

The coefficients of Eq. (3.5) and of Eq. (3.4) are functions of the turbulent Reynolds number. In the present study they were determined on the basis of handling experimental data of measurements of turbulence structure in tubes [13] and boundary layers [14, 15]. Included were experimental data of investigating decay of homogeneous turbulence behind a lattice [16], when the turbulent Reynolds number varies in a wide region. The data obtained for the closure coefficients C_1, C_2, C_μ, σ_ε were in total agreement with the results of [12].

The $e-\varepsilon$ model closed by means of these coefficients does not allow, however, to calculate the boundary layer parameters near the surface flow. The profiles of mean and fluctuating flow characteristics, obtained by a calculation by this model, do not agree with the experimental data. Moreover, the calculation leads to negative values of turbulence intensities and of dissipation for $y_* < 3$. The reason for the deviation is that Eq. (3.5) was derived under the assumption of existence of conditions of locally isotropic turbulence, which are destroyed in the boundary region, where the turbulent Reynolds numbers are small, and, consequently, does not take into account the variation of fluctuating momentum transfer near the wall.

The quantity ε can be considered as the isotropic part of the total dissipation D. From the experimental data it has been established [17] that the total dissipation vanishes at the wall. Account of this fact can be either given by corresponding boundary conditions for the dissipation equation (3.5) at the wall (for $y = 0$, $\varepsilon = 2\nu(\partial\sqrt{e}/\partial y)^2$ or $\partial\varepsilon/\partial y = 0$), or introduced by the additional term $-2\mu(\partial\sqrt{e}/\partial y)^2$ in the right hand side of the turbulence intensity equation (3.2), as was suggested in [12]. However, the use of nonvanishing boundary conditions for the equation in the form (3.5) seems to be impossible. For $\varepsilon_w \neq 0$ the last term of the dissipation equation $C_2\rho\varepsilon^2/e$ loses its physical meaning in the wall region (for $y \to 0$ it tends to infinity, since $e_w = 0$). The introduction of an additional term in the turbulence intensity equation changes the equation for e and affects the results of the solution, therefore this method was suggested in [18].

Attempts to take into account features of the dissipation distribution of turbulent energy near the wall by means of a modification of the dissipation equation would be more legitimate. The first step in this direction was undertaken in [18]. In the last term of Eq. (3.5), determining the extent of dissipation decrease, one introduces an additional function, restricting its increase near the wall, and it is written in the form

$$C_2\rho\varepsilon[\varepsilon - 2\nu(\partial\sqrt{e}/\partial y)^2]/e,$$

while the boundary condition for ε at the wall is written in the form $\partial\varepsilon/\partial y = 0$. A similar modification, however, seems to affect the results of the solution not only in the boundary layer region, but also in the external regions of the boundary layer, where the gradients of the turbulence intensity can be large, particularly in the flow transition regions.

Despite the shape differences in the turbulence intensity and dissipation equations, the profile calculations of U and e by the models of [12] and [18] coincide. In this case, for correct description of the experimental e profiles in the boundary layer region ($y_* < 15$) one introduces into the dissipation equation one additional correction term $2\mu_T\nu(\partial^2 U/\partial y^2)^2$, which was not given physical justification.

In the boundary layer model suggested in the present study the turbulence intensity and dissipation equations were included without introducing additional terms. To take into account features of turbulent transfer in the boundary layer flow region, where turbulence has an anisotropic character, we introduce into the last term of Eq. (3.5) a correction function f. The purpose of introducing this term is to restrict the increase of the dissipation degradation term near the wall. Consequently, the range of variation of this function is from 0 to 1. The specific shape of the function f is determined as a result of numerical experimentation by the condition of best agreement of velocity and turbulence intensity profiles with the experimental data of [13-16] and others. These studies contain information on the profile distributions of the velocity U, the fluctuating velocity components u', v', w', and of the turbulent tangent stress <u'v'> as a function of the transverse coordinate y. In introducing these original data into the turbulence intensity equation, which simplifies substantially near the wall due to the assumption of smallness of the convective terms in comparison with the others

$$\frac{d}{dy}\left[\left(\nu - \frac{\langle u'v'\rangle}{dU/dy}\right)\frac{de}{dy}\right] - \langle u'v'\rangle\frac{dU}{dy} = \varepsilon,$$

a system of equations is obtained for the unknown function $\varepsilon(y)$, which is selected in the form of a third-order polynomial $\varepsilon(y) = a + by + cy^2 + dy^3$. As a result of solving the equations of this system by the least squares method for each series of experiments, the dissipation value is determined as a function of the coordinate y. The profiles found and the experimental data on the U, u', v', w', <u'v'> profiles are substituted into the dissipation equation (convective terms are also neglected)

$$\frac{d}{dy}\left[\left(\nu - \frac{\langle u'v'\rangle}{\sigma_\varepsilon dU/dy}\right)\frac{d\varepsilon}{dy}\right] - C_1\langle u'v'\rangle\frac{\varepsilon}{e}\left(\frac{dU}{dy}\right)^2 = C_2 f\varepsilon^2/e,$$

as a result of whose solution the dependence $f = \varphi(y_*)$ is determined:

$$f = -\exp(-10) + \exp\left(-\frac{250}{25 + y_*^3}\right).$$

It has not been possible to establish the dependence of the function f on R_T in the present study due to the substantial scatter in the data, obtained as a result of handling the various experiments.

A numerical experiment was carried out to estimate the effect of the shape of boundary conditions for dissipation on the computation accuracy in the suggested turbulence model. It has been established that for the selected shapes of turbulence intensity and dissipation equations, as well as the closure relations, the shape of the boundary conditions for ε at the wall does not affect the velocity, temperature, and turbulence intensity profiles. The U and e profiles shown in Figs. 2 and 3 were obtained by calculations by the suggested model with the use of the two boundary conditions $\varepsilon_w = 2\nu(\partial\sqrt{e}/\partial y)^2$ and $\varepsilon_w = 0$, in which case the calculated data coincided with each other, for which reason they are shown by a single solid line. The calculated dissipation profiles for both cases mentioned of boundary conditions differ only near the walls $y_* < 3$. Taking into account that in this flow region the turbulent transfer coefficient μ_T is negligibly small, while the dissipation effect on the mean flow characteristics is mostly realized precisely through it, the absence of a substantial effect of boundary conditions for ε on the calculation results becomes understandable.

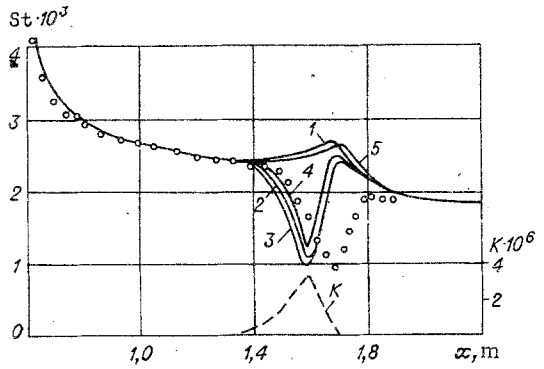

Fig. 1

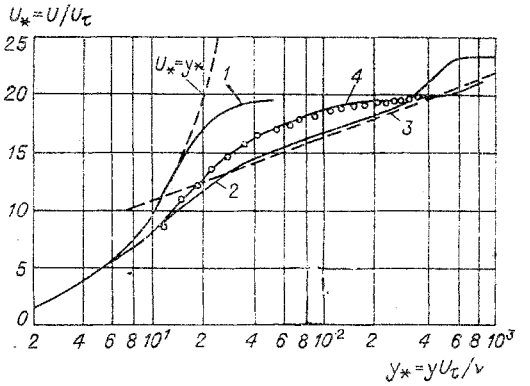

Fig. 2

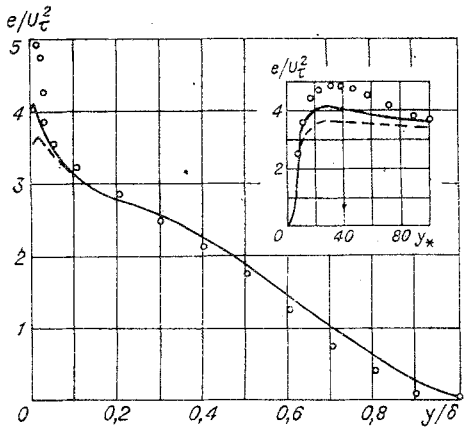

Fig. 3

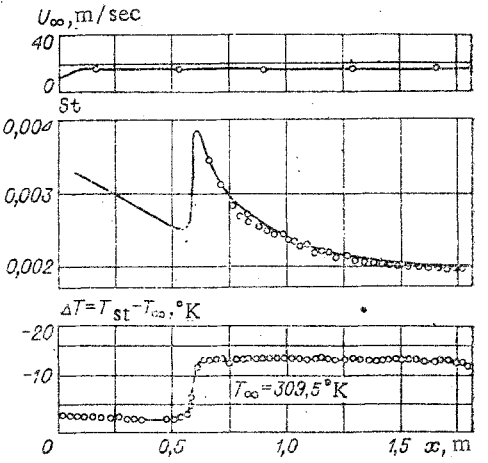

Fig. 4

The choice of the boundary condition for dissipation in the form $\varepsilon_w = 0$, and not $\varepsilon_w = 2\nu(\partial\sqrt{e}/\partial y)^2$ or $(\partial\varepsilon/\partial y)_w = 0$, is due to the fact that this homogeneous boundary condition guarantees most solution stability in enhancing the steps of the difference grid.

4. Mathematical Boundary Layer Model. The system of equations describing a turbulent boundary layer, along with the closure coefficients, are

$$\frac{\partial \rho U}{\partial x} + \frac{\partial \rho V}{\partial y} = 0, \quad \rho U\frac{\partial U}{\partial x} + \rho V\frac{\partial U}{\partial y} = \frac{\partial}{\partial y}\left[(\mu + \mu_т)\frac{\partial U}{\partial y}\right] - \frac{dp}{dx},$$

$$C_p\rho U\frac{\partial T}{\partial x} + C_p\rho V\frac{\partial T}{\partial y} = \frac{\partial}{\partial y}\left[(\lambda + \lambda_т)\frac{\partial T}{\partial y}\right] + U\frac{dp}{dx} + \mu\left(\frac{\partial U}{\partial y}\right)^2 + \rho\varepsilon,$$

$$\rho U\frac{\partial e}{\partial x} + \rho V\frac{\partial e}{\partial y} = \frac{\partial}{\partial y}\left[(\mu + \mu_т)\frac{\partial e}{\partial y}\right] + \mu_т\left(\frac{\partial U}{\partial y}\right)^2 - \rho\varepsilon, \tag{4.1}$$

$$\rho U\frac{\partial \varepsilon}{\partial x} + \rho V\frac{\partial \varepsilon}{\partial y} = \frac{\partial}{\partial y}\left[\left(\mu + \frac{\mu_т}{\sigma_\varepsilon}\right)\frac{\partial \varepsilon}{\partial y}\right] + C_1\mu_т\frac{\varepsilon}{e}\left(\frac{\partial U}{\partial y}\right)^2 - C_2 f\frac{\rho\varepsilon^2}{e},$$

$$C_1 = 1.65, \quad C_2 = 2\left[1 - 0.3\exp\left(-R_т^2\right)\right], \quad \sigma_\varepsilon = 1.3,$$

$$C_\mu = 0.09\left[-\exp(-2.5) + \exp\left(-\frac{125}{50 + R_т}\right)\right], \quad f = -\exp(-10) + \exp\left(-\frac{250}{25 + y_*^3}\right),$$

where x and y are the rectangular coordinates, respectively, along and across the flow, U and V are the mean velocity components, $e = \frac{1}{2}\sum_{i=1}^{3}\langle(u_i')^2\rangle$ is the turbulence intensity, T is the mean temperature, u_i' are the components of the fluctuating velocity, $\varepsilon = \nu\sum_{i,j=1}^{3}\langle(\partial u_i'/\partial x_j)^2\rangle$ is

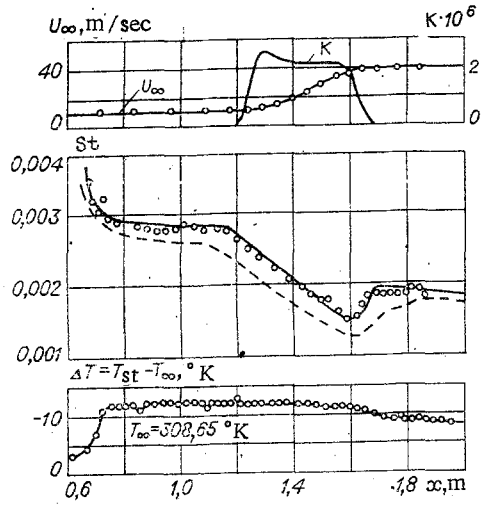

Fig. 5

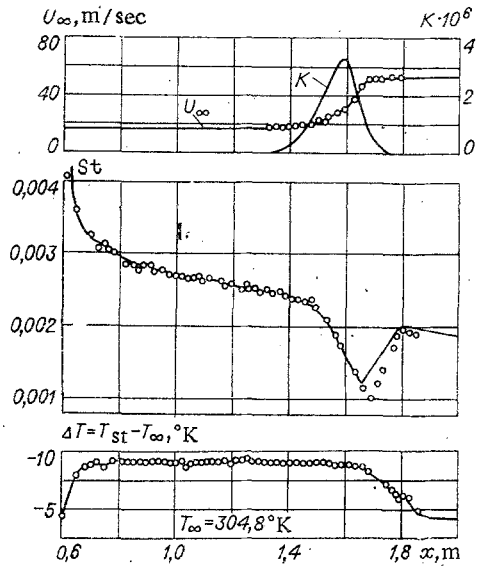

Fig. 6

the dissipation, C_1, C_2, C_μ, and σ_ε are empirical coefficients, and $y_* = y\sqrt{\tau_w/\rho}/\nu$ is a dimensionless transverse coordinate.

The corresponding boundary conditions are taken in the form

$$y = 0,\ U = V = e = \varepsilon = 0,\ T = T_w(x),$$
$$y \to \infty,\ \partial U/\partial y = \partial T/\partial y = \partial e/\partial y = \partial \varepsilon/\partial y = 0. \qquad (4.2)$$

Equations (4.1), (4.2), together with the equation of state and the relations $\mu = \mu(p, T)$, $\lambda = \lambda(p, T)$, $C_p = C_p(p, T)$, $R = R(p, T)$ were solved by computer. The original equations and the boundary conditions were approximated by means of finite-difference analogs, written in an implicit scheme. The initial profiles were assigned by the experimental data for the laminar and turbulent flow regimes [19]. The system of linear equations obtained in this case was solved numerically. To accelerate the computational process and guarantee its accuracy we introduced a modified system of coordinates, guaranteeing "compression" of the transverse coordinate near the wall. Satisfactory computational accuracy was achieved for nongradient flow regimes for 40, and for accelerated flow for 100 points across the computational grid.

5. Calculation Results. With the purpose of estimating the validity of the mathematical boundary layer model proposed we calculated velocity profiles for various flow regimes. A solution was realized, starting at some point of a planar plate in which $Re_x \sim 10^4$, and the relative amount of turbulence of the running flow did not exceed 0.5%. Under these conditions the boundary layer has a laminar character (curve 1 of Fig. 2 was obtained for $Re_x = 10^5$, $K = 0$). When leaving the turbulent flow regime, the calculated profile of the mean velocity is changed (curve 2 in Fig. 2, $Re_x = 4 \cdot 10^5$, $K = 0$), and coincides with the logarithmic distribution law $U_* = 5.5 \log y_* + 5.45$ (curve 3). In the action zone of accelerated flow the calculated velocity profile (curve 4, $Re_x = 1.5 \cdot 10^6$, $K = 2.2 \cdot 10^{-6}$) is inclined toward laminar profiles and coincides with the experimental data [12] for $K = 2.2 \cdot 10^{-6}$.

Figure 3 shows a comparison of turbulence intensity profiles across the boundary layer on a planar plate, calculated by means of the present model (the solid curve) and by the model of [12] (dashed curve), with the experimental data [14] for $Re_x = 4.2 \cdot 10^6$ (points). In the wall region the calculated profiles are below the experimental values, but the calculation by the proposed model provides better agreement with experiment. For $y/\delta > 0.1$ the calculated profiles coincide totally, therefore, they are shown in the figure by a single solid line.

The possibilities of the suggested model in describing heat transfer in a turbulent boundary layer were estimated in comparison with experimental data [1] (points). As boundary conditionsin the calculation we used the flow velocity, as well as the temperature difference between the wall and the external flow, obtained experimentally. It follows from Fig. 4 that the calculated Stanton number for the case of the gradientless flow regime ($K = 0$) coincides with experimental data.

In the case of moderate flow accelerations ($K_{max} = 2.52 \cdot 10^{-6}$), acting along a significant distance of the investigated surface, the calculation describes accurately the lowering region of heat transfer intensity. The continuous and dashed lines in Fig. 5 show calculation results by the proposed model and by the model of [12], respetively. Obviously, the calculation by the model of [12] gives substantially worse agreement with experiment.

As follows from Fig. 6, when the flow acceleration has a short-term peak character, the calculation accuracy is lowered, but the model makes it possible to estimate correctly the lowered intensity of heat transfer.

LITERATURE CITED

1. P. M. Moretti and W. W. Kays, "Heat transfer to a turbulent boundary layer with varying free-stream velocity and varying surface temperature — an experimental study," Int. J. Heat Mass Transfer, 8, No. 9 (1965).
2. M. A. Badri Naraynan, "An experimental study of reverse transition in two-dimensional channel flow," J. Fluid Mech., 31, No. 3 (1968).
3. B. E. Launder and D. B. Spalding, Mathematical Models of Turbulence, Academic Press (1972).
4. T. Cebeci, A. M. O. Smith, and G. J. Mosinskis, "Solution of the incompressible turbulent boundary layer equations with heat transfer," J. Heat Transfer, 92, 113 (1970).
5. W. M. Kays, "Heat transfer to the transpired turbulent boundary layer," Int. J. Heat Mass Transfer, 15, No. 5 (1972).
6. B. E. Launder and W. P. Jones, "Sink flow turbulent boundary layers," J. Fluid Mech., 38, No. 4 (1969).
7. R. F. Blackwelder and L. S. G. Kovasznay, "Large-scale motion of a turbulent boundary layer during relaminarization," J. Fluid Mech., 53, No. 1 (1972).
8. A. N. Kolmogorov, "Equations of turbulent motion of an incompressible fluid," Izv. Akad. Nauk SSSR, Ser. Fiz., 6, No. 1-2 (1942).
9. L. Prandtl, "A new system of equations for structured turbulence," Nach. Akad. Wissen. Göttingen, p. 6 (1945).
10. A. N. Kolmogorov, "Local structure of turbulence in an incompressible fluid for very large Reynolds numbers," Dokl. Akad. Nauk SSSR, 30, No. 4 (1941).
11. B. N. Davydov, "Statistical dynamics of an incompressible turbulent fluid," Dokl. Akad. Nauk SSSR, 136, No. 1 (1961).
12. W. B. Jones and B. E. Launder, "The prediction of laminarization with a two-equation model of turbulence," Int. J. Heat Mass Transfer, 15, No. 2 (1972).
13. J. Laufer, "The structure of turbulence in fully developed pipe flow," Rept. NACA No. 1174 (1954).
14. P. S. Klebanoff, "Characteristics of turbulence in a boundary layer with zero pressure gradient," Rept. NACA No. 1247 (1955).
15. P. Bradshaw, "The turbulence structure of equilibrium boundary layers," J. Fluid Mech., 29, No. 4 (1967).
16. A. A. Townsend, The Structure of Turbulent Shear Flow, Cambridge University Press (1976).
17. I. K. Rotta, Turbulent Boundary Layers in Incompressible Fluids [in Russian], Sudostroenie, Leningrad (1967).
18. K. Hanjalic and B. E. Launder, "Contribution towards a Reynolds-stress closure for low-Reynolds-number turbulence," J. Fluid Mech., 74, No. 4 (1976).
19. J. G. Hinze, Turbulence, McGraw-Hill, New York (1975).